Time domain homogenization of metamaterials

Mário G. Silveirinha[*]

University of Coimbra, Department of Electrical Engineering, Instituto de Telecomunicações, 3030 Coimbra, Portugal
(Received 13 December 2010; revised manuscript received 27 January 2011; published 7 April 2011)

We propose a simple, robust, and versatile time domain approach to homogenize metamaterials, taking into account both frequency and spatial dispersion. The macroscopic electromagnetic response of optical metamaterials, such as the fishnet structure and plasmonic metamaterials with near zero parameters, is characterized in terms of local effective parameters ε and μ, under the assumption that the effects of spatial dispersion are weak.

I. INTRODUCTION

Metamaterials are mesoscopic structures whose electromagnetic response in the long-wavelength limit is mainly determined by artificially built-in features, and not directly by the chemical composition. Such features effectively define a new length scale in the system, and consequently enable the emergence of exotic physical phenomena such as negative refraction,[1] low loss broadband anomalous dispersion,[2] and artificial magnetism.[3]

It is very convenient to describe the propagation of electromagnetic waves in metamaterials using effective medium theories. This enables reducing the inherent microscopic complexity of the material to a few effective parameters, usually an equivalent permittivity and permeability, making an otherwise very intricate problem easily accessible to theoretical modeling. Such an approach is physically sound when the wavelength of the radiation is much longer than the characteristic features of the metamaterial, so that the intrinsic granularity of the system can be neglected, and the structure can be regarded as a continuous effective medium.

Different homogenization techniques have been proposed over the years to characterize composite media, e.g. Refs. 4–13. In particular, a few years ago this author proposed a fully self-consistent homogenization method to characterize periodic metamaterials formed by dielectric or metallic particles of arbitrary shapes and material parameters, taking into account both the effects of frequency and spatial dispersion. Within this formalism, the medium is characterized by a dielectric function $\overline{\overline{\varepsilon}}_{\text{eff}}(\omega,\mathbf{k})$, which completely determines the effective response of the medium to an external excitation with a space-time variation of the type $e^{-i\omega t}e^{i\mathbf{k}\cdot\mathbf{r}}$(the macroscopic response for an excitation with an arbitrary space-time dependence, e.g., a localized source embedded in the medium, can be determined using Fourier theory).[4,5,14,15] In previous works, it was shown how the effective dielectric function can be numerically computed using the method of moments (MoM) (based on a periodic Green function)[4] and the finite difference frequency domain (FDFD) method.[5] However, the MoM and integral equation methods are difficult to apply to dielectric structures and are mainly appropriate when the inclusions are perfect electric conductors. On the other hand, the FDFD method requires solving an $N \times N$ linear system (N being proportional to the number of nodes in the mesh), which is inefficient and often computationally prohibitive in the case of complex three-dimensional systems.

In this work, we develop a homogenization algorithm based on the finite difference time domain (FDTD) (Ref. 16) method originally introduced by Yee[17] to compute the effective dielectric function of periodic metamaterials. Our solution has the typical advantages of the FDTD method:[16] (i) It is an order-N method, i.e., the computational effort scales linearly with the size of the system. (ii) The update equations for the fields are fully explicit and so the method requires neither solving a linear system (as the FDFD method), nor evaluating complex integrals involving functions with singularities (as the MoM). (iii) It can be applied to both dielectric and metallic systems and it is very simple to implement computationally and suitable for parallelization (parallel computing).

This paper is organized as follows. In Sec. II, we present the theoretical background. In Sec. III, we describe the FDTD implementation of the homogenization problem. In Sec. IV, several numerical examples that illustrate the application of the method are given. Finally, in Sec. V, the conclusions are drawn.

II. THEORETICAL BACKGROUND

The homogenization approach introduced in Ref. 4 is based on the idea of using an external excitation to compute the effective parameters of a metamaterial. The external excitation must be macroscopic so that it remains invariant after spatial averaging. Specifically, for given ω and $\mathbf{k}$, the dielectric function $\overline{\overline{\varepsilon}}_{\text{eff}}(\omega,\mathbf{k})$ is computed by exciting the periodic structure with a density of electric current of the form $\mathbf{j}_e = \mathbf{j}_{e,\text{av}} e^{i\mathbf{k}\cdot\mathbf{r}}$ where $\mathbf{j}_{e,\text{av}}$ is a constant vector. Since $\mathbf{j}_{e,\text{av}}$ can be oriented along three different directions of space, it is necessary to consider three distinct sources (three linearly independent vectors $\mathbf{j}_{e,\text{av}}$). For each of the sources, the induced microscopic fields are determined by solving Maxwell's equations.[4,5] Next, the microscopic electric field $\mathbf{e}$ and the microscopic polarization vector $\mathbf{p} = (\varepsilon - \varepsilon_0)\mathbf{e}$ are spatially averaged; $\mathbf{E}_n = \langle \mathbf{e}_n \rangle$ and $\mathbf{P}_{g,n} = \langle \mathbf{p}_n \rangle$, where $n = 1,2,3$ labels the fields associated with one specific excitation $\mathbf{j}_{e,\text{av}}$ and $\langle \rangle$ represents the averaging operator (in this work, the microscopic fields are denoted with lower case letters and the macroscopic fields are denoted with upper case letters). Finally, $\overline{\overline{\varepsilon}}_{\text{eff}}(\omega,\mathbf{k})$ is defined in such a way that $(\overline{\overline{\varepsilon}}_{\text{eff}} - \varepsilon_0\overline{\overline{\mathbf{I}}}) \cdot \mathbf{E}_n = \mathbf{P}_{g,n}$ for $n = 1,2,3$. The effective dielectric function is independent of the excitations $\mathbf{j}_{e,\text{av}}$ that are considered.

The spatial averaging procedure adopted in Ref. 4 is equivalent to ideal low pass filtering.[14,15] Thus, for example, if the microscopic electric field is a Bloch wave associated with the wave vector $\mathbf{k}$ (assumed to be within the first Brillouin zone), we have $\langle \mathbf{e} \rangle = \mathbf{E}_{\text{av}} e^{i\mathbf{k}\cdot\mathbf{r}}$ where

$$\mathbf{E}_{\text{av}} = \frac{1}{V_{\text{cell}}} \int_{\Omega} \mathbf{e}(\mathbf{r}) e^{-i\mathbf{k}\cdot\mathbf{r}} d^3\mathbf{r} \qquad (1)$$

V_{cell} being the volume of the unit cell Ω. Note that in this work we adopt a convention $e^{i\mathbf{k}\cdot\mathbf{r}} e^{-i\omega t}$ in the spectral domain, whereas in Refs. 4 and 5, we used instead $e^{-j\mathbf{k}\cdot\mathbf{r}} e^{j\omega t}$.

In Ref. 4 the homogenization problem was formulated directly in the frequency domain. However, evidently, it is also possible to formulate it in the time domain. In order to show this, let us suppose that the metamaterial is characterized at the microscopic level by a frequency independent permittivity $\varepsilon_s(\mathbf{r})$. The general case where the permittivity is frequency dependent is discussed in the Appendix.

In the time domain, the Maxwell's equations in the periodic structure (assuming that all the materials are nonmagnetic) can be written as

$$\nabla \times \mathbf{e} = -\mu_0 \frac{\partial \mathbf{h}}{\partial t}, \qquad (2a)$$

$$\nabla \times \mathbf{h} = \mathbf{j}_e + \varepsilon_s(\mathbf{r}) \frac{\partial \mathbf{e}}{\partial t}. \qquad (2b)$$

In order to evaluate $\overline{\overline{\varepsilon}}_{\text{eff}}(\omega, \mathbf{k})$ for a given wave vector $\mathbf{k} = (k_x, k_y, k_z)$ we propose to solve the system (2) in the time domain with trivial initial time boundary conditions,

$$\mathbf{e}(\mathbf{r}, t = 0) = 0; \quad \mathbf{h}(\mathbf{r}, t = 0) = 0 \qquad (3)$$

and with an external source of the form

$$\mathbf{j}_e(\mathbf{r}, t) = \hat{\mathbf{u}}_n e^{i\mathbf{k}\cdot\mathbf{r}} g(t) \quad (\text{n} = 1, 2, 3), \qquad (4)$$

where $g(t)$ is some suitable function of time (e.g., a Gaussian pulse) and $\hat{\mathbf{u}}_n$ is a unit vector directed along one of the coordinate axes. It is worth noting that in general the solution of Eq. (2) is complex valued because the excitation also is. Moreover, due to the periodicity of the metamaterial, for every t fixed the microscopic fields are clearly Bloch modes associated with the wave vector $\mathbf{k}$. Therefore the computational domain can always be reduced to a unit cell.

We also note that the spatially averaged electric field and polarization vector in the time domain are of the form $\langle \mathbf{e} \rangle = \mathbf{E}_{\text{av}}(t) e^{i\mathbf{k}\cdot\mathbf{r}}$ and $\langle \mathbf{p} \rangle = \mathbf{P}_{g,\text{av}}(t) e^{i\mathbf{k}\cdot\mathbf{r}}$ with

$$\mathbf{E}_{\text{av}}(t) = \frac{1}{V_{\text{cell}}} \int_{\Omega} \mathbf{e}(\mathbf{r}, t) e^{-i\mathbf{k}\cdot\mathbf{r}} d^3\mathbf{r}, \qquad (5a)$$

$$\mathbf{P}_{g,\text{av}}(t) = \frac{1}{V_{\text{cell}}} \int_{\Omega} (\varepsilon_s - \varepsilon_0) \mathbf{e}(\mathbf{r}, t) e^{-i\mathbf{k}\cdot\mathbf{r}} d^3\mathbf{r}. \qquad (5b)$$

In order to see how $\overline{\overline{\varepsilon}}_{\text{eff}}(\omega, \mathbf{k})$ can be obtained from the solution of Eq. (2), let us calculate the unilateral Laplace transform of the microscopic fields. The Laplace transform is denoted with the symbol "$\sim$" so that the Laplace transform of the electric field (for example) is

$$\tilde{\mathbf{e}}(\mathbf{r}, s) = \int_0^{+\infty} \mathbf{e}(\mathbf{r}, s) e^{-st} dt. \qquad (6)$$

Because of the passivity of all materials, the region of convergence of the Laplace transform includes always the semiplane $\text{Re}(s) > 0$.

Since the Laplace transform of $\partial f / \partial t$ is $\tilde{f}(s)s - f(0)$, it follows that (using the fact that $\mathbf{e} = 0$ and $\mathbf{h} = 0$ for $t = 0$)

$$\nabla \times \tilde{\mathbf{e}} = -\mu_0 s \tilde{\mathbf{h}}, \qquad (7a)$$

$$\nabla \times \tilde{\mathbf{h}} = \hat{\mathbf{u}}_n e^{i\mathbf{k}\cdot\mathbf{r}} \tilde{g}(s) + s \varepsilon_s \tilde{\mathbf{e}}. \qquad (7b)$$

Thus it should be clear that $\tilde{\mathbf{e}}$ and $\tilde{\mathbf{h}}$ evaluated for $s = -i\omega$ are the solutions of the homogenization problem formulated in Ref. 4. Hence we conclude that $\overline{\overline{\varepsilon}}_{\text{eff}}(\omega, \mathbf{k})$ can be determined from $\langle \tilde{\mathbf{e}}_n \rangle$ and $\langle \tilde{\mathbf{p}}_n \rangle$, evaluated for $s = -i\omega$, where $n = 1, 2, 3$ labels the considered excitation (external current along $\hat{\mathbf{u}}_n$). It is obvious that

$$\langle \tilde{\mathbf{e}} \rangle = \tilde{\mathbf{E}}_{\text{av}}(s) e^{i\mathbf{k}\cdot\mathbf{r}}, \quad \langle \tilde{\mathbf{p}} \rangle = \tilde{\mathbf{P}}_{g,\text{av}}(s) e^{i\mathbf{k}\cdot\mathbf{r}}, \qquad (8)$$

where $\mathbf{E}_{\text{av}}(t)$ and $\mathbf{P}_{g,\text{av}}(t)$ are defined as in Eq. (5). Hence for a given $\mathbf{k}$, we can use the following algorithm to compute $\overline{\overline{\varepsilon}}_{\text{eff}}(\omega, \mathbf{k})$:

(i) For $n = 1, 2, 3$, solve the time domain problem defined by system (2), subject to trivial initial time boundary conditions and an external excitation as in Eq. (4). The electric field solution of each of these time domain source driven problems is denoted by $\mathbf{e}_n$.

(ii) For $n = 1, 2, 3$, determine the spatially averaged electric field $\mathbf{E}_{\text{av},n}(t)$ and the spatially averaged polarization vector $\mathbf{P}_{g,\text{av},n}(t)$ defined as in Eq. (5).

(iii) For $n = 1, 2, 3$, calculate the Laplace transforms of $\mathbf{E}_{\text{av},n}(t)$ and $\mathbf{P}_{g,\text{av},n}(t)$, i.e., calculate $\tilde{\mathbf{E}}_{\text{av},n}(s)$ and $\tilde{\mathbf{P}}_{g,\text{av},n}(s)$.

(iv) The unknown dielectric function $\overline{\overline{\varepsilon}}_{\text{eff}}(\omega, \mathbf{k})$ is such that $(\overline{\overline{\varepsilon}}_{\text{eff}} - \varepsilon_0 \overline{\overline{\mathbf{I}}}) \cdot \tilde{\mathbf{E}}_{\text{av},n} = \tilde{\mathbf{P}}_{g,n}$ for $n = 1, 2, 3$, where $\tilde{\mathbf{E}}_{\text{av},n}$ and $\tilde{\mathbf{P}}_{g,n}$ are evaluated for $s = -i\omega$.

Some notes are in order at this point. First of all, it should be clear that for a given $\mathbf{k}$ the dielectric function $\overline{\overline{\varepsilon}}_{\text{eff}}$ is computed simultaneously for all frequencies, i.e., for all ω. Moreover, the computed $\overline{\overline{\varepsilon}}_{\text{eff}}$ is completely independent of $g(t)$, i.e., of the dependence in time of the excitation [see Eq. (4)]. As discussed later, in practice $g(t)$ is chosen so that its frequency spectrum is concentrated in the frequency range of interest.

Another important aspect is that in a lossless scenario, for example, if the inclusions are dielectrics with no dispersion as considered in this section, there is no absorption loss. Moreover, due to the Bloch boundary conditions, there is also no radiation loss, and thus the electromagnetic fields do not die out, even when the excitation is switched off. In practice this implies that the region of convergence of the Laplace transform is the semiplane $\text{Re}\{s\} > 0$. Indeed, the system has its poles in the imaginary axis $\text{Re}\{s\} = 0$. This is obviously an inconvenience because for ω real valued, $s = -i\omega$ is over the imaginary axis, which is outside the region of convergence of the Laplace transform. Nevertheless, it is possible to circumvent this problem by considering that $\omega = \omega' + i\omega''$ where ω'' should be ideally an infinitesimally small positive number. Thus in practice $\overline{\overline{\varepsilon}}_{\text{eff}}$ will be evaluated for a complex valued frequency (in the upper half plane and very close to the real axis). The computational implications of this fact will be discussed in the next section.

It is interesting to note that a similar strategy to achieve convergence is used in Ref. 18, which deals with the computation

of the photonic Green's function using the FDTD method. Moreover, our time domain problem [Eq. (2)] is formally equivalent to that considered within the framework of the so-called N-order method[18,19] to calculate the band structure of photonic crystals. However, here we compute the average fields to determine the dielectric function, whereas in Ref. 19 the authors identify the spectral resonances to calculate the band-structure diagram. In particular, an FDTD implementation of the N-order method can be easily adapted to solve the homogenization problem considered here.

There is also another difference between the N-order method and system (2): In our formulation we consider trivial initial time boundary conditions and an external excitation, whereas in Ref. 19 there is no external excitation and the initial time electric and magnetic fields are nonzero. Actually this difference is not really relevant, because it is possible as well to compute $\overline{\overline{\varepsilon}}_{\text{eff}}$ by assuming that there is no external excitation [$\mathbf{j}_e(\mathbf{r},t) = 0$] and that the initial time boundary condition for the electric field is nontrivial $\mathbf{e}(\mathbf{r},t=0) \neq 0$. Indeed, in such scenario the Laplace transforms of the time domain fields would satisfy [compare with (7b)]

$$\nabla \times \tilde{\mathbf{h}} = -\varepsilon_s(\mathbf{r})\mathbf{e}(\mathbf{r},t=0) + s\varepsilon_s(\mathbf{r})\tilde{\mathbf{e}}. \qquad (9)$$

Thus it is simple to verify that if the initial time boundary condition is chosen in such a way that $\varepsilon_s(\mathbf{r})\mathbf{e}(\mathbf{r},t=0) \sim \hat{\mathbf{u}}_n e^{i\mathbf{k}\cdot\mathbf{r}}$ and $\mathbf{h}(\mathbf{r},t=0) = 0$ then $\overline{\overline{\varepsilon}}_{\text{eff}}$ can be still calculated using exactly the same algorithm as that delineated before, but using $\mathbf{j}_e(\mathbf{r},t) = 0$. Thus from a computational point of view, our time domain homogenization approach is, indeed, related to the N-order method of Ref. 19.

III. FDTD SOLUTION OF THE HOMOGENIZATION PROBLEM

In the following, we briefly describe the FDTD implementation of system (2), and discuss how the function $g(t)$ that determines the time dependence of the excitation should be chosen, as well as the duration of the simulation and the time step.

A. Discretization of Maxwell's equations

The FDTD discretization of system (2) is done in a completely standard way.[16] As mentioned before, the computational domain can always be taken equal to the unit cell of the metamaterial. Assuming that unit cell is simple orthorhombic, e.g., $\Omega = [0,a_x] \times [0,a_y] \times [0,a_z]$, the grid nodes can be chosen equal to (considering uniform meshing along which coordinate axes)

$$(x_i, y_j, z_k) = \left(a_x \frac{i-1}{N_x}, a_y \frac{j-1}{N_y}, a_z \frac{k-1}{N_z} \right),$$
$$1 \leqslant i \leqslant N_x, 1 \leqslant j \leqslant N_y \text{ and } 1 \leqslant k \leqslant N_z \qquad (10)$$

where N_x is the number of nodes along the x direction, and N_y and N_z are defined similarly. Following the usual approach, the point (x_i, y_j, z_k) is simply denoted by (i,j,k). The distance between two consecutive nodes along the x direction is evidently $\Delta_x = a_x/N_x$. The parameters Δ_y and Δ_z are defined

similarly. We use the shorthand notation $(i \pm \frac{1}{2}, j, k)$ to denote the grid points $(x_i \pm \Delta_x/2, y_j, z_k)$, etc.

In the FDTD method the spatial components of the electric and magnetic fields are spatially staggered so that each electric- (magnetic-) field component is located midway between a pair of magnetic- (electric-) field components.[17] Specifically, the electric-field components may be defined over the nodes indicated below:

$$e_x \to e_x\left(i + \tfrac{1}{2}, j, k\right), \quad e_y \to e_y\left(i, j + \tfrac{1}{2}, k\right),$$
$$e_z \to e_z\left(i, j, k + \tfrac{1}{2}\right) \qquad (11)$$

whereas the magnetic-field components are defined over the nodes,

$$h_x \to h_x\left(i, j + \tfrac{1}{2}, k + \tfrac{1}{2}\right), h_y \to h_y\left(i + \tfrac{1}{2}, j, k + \tfrac{1}{2}\right),$$
$$h_z \to h_z\left(i + \tfrac{1}{2}, j + \tfrac{1}{2}, k\right) \qquad (12)$$

with $1 \leqslant i \leqslant N_x, 1 \leqslant j \leqslant N_y$ and $1 \leqslant k \leqslant N_z$. This meshing scheme was originally proposed by Yee[17] and enables replacing spatial derivatives by central differences. For example, one may approximate the z component of Eq. (2a) by

$$\frac{\partial h_z}{\partial t}\left(i + \frac{1}{2}, j + \frac{1}{2}, k, t\right)$$
$$= -\frac{1}{\mu_0}\left(\frac{e_y\left(i+1, j+\tfrac{1}{2}, k, t\right) - e_y\left(i, j+\tfrac{1}{2}, k, t\right)}{\Delta_x}\right.$$
$$\left. -\frac{e_x\left(i+\tfrac{1}{2}, j+1, k, t\right) - e_x\left(i+\tfrac{1}{2}, j, k, t\right)}{\Delta_y}\right). \qquad (13)$$

Whenever a given node lies outside the grid it can always be brought back using the Bloch-Floquet boundary conditions. For example,

$$e_x\left(i + \tfrac{1}{2}, j, N_z + 1\right) = e_x\left(i + \tfrac{1}{2}, j, 1\right)e^{ik_z a_z}. \qquad (14)$$

In the FDTD method the time derivatives are also approximated by finite differences. Moreover, the time nodes for the electric and magnetic are staggered in time, so that the electric- (magnetic-) field updates are taken in the middle of consecutive magnetic- (electric-) field updates. This leapfrog scheme was proposed by Yee,[17] and enables updating explicitly the values of the fields (without requiring solving a linear system), in a marching in time procedure that mimics the propagation of electromagnetic waves in an actual physical system. Denoting $e_i(x,y,z,n\Delta_t)$ by $e_i^n(x,y,z)$ and $h_i[x,y,z,(n\pm\tfrac{1}{2})\Delta_t]$ by $h_i^{n\pm1/2}(x,y,z)$, where Δ_t is the time

step, it follows that Eq. (13) can be written as

$$
\begin{aligned}
h_z^{n+1/2}&\left(i+\frac{1}{2},j+\frac{1}{2},k\right)\\
&= h_z^{n-1/2}\left(i+\frac{1}{2},j+\frac{1}{2},k\right) - \frac{\Delta_t}{\mu_0}\left(\frac{e_y^n\left(i+1,j+\frac{1}{2},k\right)-e_y^n\left(i,j+\frac{1}{2},k\right)}{\Delta_x} - \frac{e_x^n\left(i+\frac{1}{2},j+1,k\right)-e_x^n\left(i+\frac{1}{2},j,k\right)}{\Delta_y}\right). \quad (15)
\end{aligned}
$$

The x and y components of Eq. (2a) are discretized in the same manner. On the other hand, the z component of Eq. (2b) can be discretized as follows:

$$
\begin{aligned}
e_z^{n+1}\left(i,j,k+\frac{1}{2}\right) = {}& e_z^n\left(i,j,k+\frac{1}{2}\right) + \frac{\Delta_t}{\varepsilon_s\left(i,j,k+\frac{1}{2}\right)}\Bigg[-j_{e,z}^{n+1/2}\left(i,j,k+\frac{1}{2}\right)\\
&+ \frac{h_y^{n+1/2}\left(i+\frac{1}{2},j,k+\frac{1}{2}\right)-h_y^{n+1/2}\left(i-\frac{1}{2},j,k+\frac{1}{2}\right)}{\Delta_x}\\
&- \frac{h_x^{n+1/2}\left(i,j+\frac{1}{2},k+\frac{1}{2}\right)-h_x^{n+1/2}\left(i,j-\frac{1}{2},k+\frac{1}{2}\right)}{\Delta_y}\Bigg]. \quad (16)
\end{aligned}
$$

The x and y components of the same equation can be discretized similarly. Using the update expressions (15) and (16) (and the corresponding update formulas for the x and y components of the fields), it is possible to determine the time evolution of the electromagnetic field for vanishing initial time boundary conditions and a given source $\mathbf{j}_e$.

In order to determine the effective dielectric function $\overline{\overline{\varepsilon}}_{\text{eff}}(\omega,\mathbf{k})$ it is necessary to evaluate and store at each time step the averaged electric field and polarization vector. The z components of these vectors are calculated at the nth time step as follows (the x and y components are obtained analogously):

$$
E_{\text{av},z}^n \equiv E_{\text{av},z}(n\Delta_t) = \frac{\Delta_x\Delta_y\Delta_z}{V_{\text{cell}}}\sum_{i,j,k} e_z^n\left(i,j,k+\frac{1}{2}\right)e^{-i\mathbf{k}\cdot(x_i,y_j,z_k+\Delta_z/2)}, \quad (17a)
$$

$$
P_{\text{g},\text{av},z}^n \equiv P_{\text{g},\text{av},z}(n\Delta_t) = \frac{\Delta_x\Delta_y\Delta_z}{V_{\text{cell}}}\sum_{i,j,k}\left[\varepsilon_s\left(i,j,k+\frac{1}{2}\right)-\varepsilon_0\right]e_z^n\left(i,j,k+\frac{1}{2}\right)e^{-i\mathbf{k}\cdot(x_i,y_j,z_k+\Delta_z/2)}. \quad (17b)
$$

When the FDTD simulation is concluded (after a sufficiently large number of time steps; see the next subsection), one should have the values of $\mathbf{E}_{\text{av}}^n$ and $\mathbf{P}_{g,\text{av}}^n$ stored in memory for every time step n. At this point it is possible to determine the Laplace transforms of $\mathbf{E}_{\text{av}}$ and $\mathbf{P}_{g,\text{av}}$ calculated at $s = -i\omega$. Assuming that $\omega = \omega' + i\omega''$, these can be discretized as follows:

$$
\tilde{\mathbf{E}}_{\text{av}}(\omega) = \Delta_t \sum_n \mathbf{E}_{\text{av}}^n e^{-\omega'' n\Delta_t} e^{+i\omega' n\Delta_t}. \quad (18)
$$

$\tilde{\mathbf{P}}_{g,\text{av}}$ is defined similarly. In practice, as discussed in Sec. II, one chooses ω'' as some small positive number and evaluates $\tilde{\mathbf{E}}_{\text{av}}$ and $\tilde{\mathbf{P}}_{g,\text{av}}$ at the frequencies ω' for which one wants to determine $\overline{\overline{\varepsilon}}_{\text{eff}}(\omega,\mathbf{k})$. For a sequence of values of the form $\omega' = 2\pi l/\Delta_t$, with l integer, summation (18) can be efficiently evaluated using the fast Fourier transform (FFT). Once $\tilde{\mathbf{E}}_{\text{av}}$ and $\tilde{\mathbf{P}}_{g,\text{av}}$ are known for three different excitations, the nonlocal dielectric function can be determined as explained in the previous section.

B. Time step and time profile of the excitation

The time profile $g(t)$ of the excitation should be such that its spectral content is concentrated in the frequency window $\omega_{\text{min}} < \omega < \omega_{\text{max}}$ where we are interested in calculating the effective parameters. A suitable choice is a Gaussian pulse of the form

$$
g(t) = \sin(\omega_0 t)\exp\left[-(t-t_m)^2/\sigma_g^2\right], \quad t > 0. \quad (19)
$$

The parameter ω_0 may be chosen as $\omega_0 = (\omega_{\text{min}} + \omega_{\text{max}})/2$, and the parameters σ_g and t_m should be such that $\sigma_g \sim 2/(\omega_{\text{max}} - \omega_{\text{min}})$ and $t_m \sim 3\sigma_g$.

The time step Δ_t should be consistent with the well-known stability criterion:[16,20]

$$
\Delta_t < \frac{1}{c}\left(\frac{1}{\Delta_x^2} + \frac{1}{\Delta_y^2} + \frac{1}{\Delta_z^2}\right)^{-1/2}. \quad (20)
$$

In our simulations we used $\Delta_t \sim \Delta_{t,\text{max}}/1.5$. Finally, the duration of the time simulation, t_{max}, is determined by both ω'' (which must be different from zero to ensure the convergence

of the homogenization method) and by $\omega_{\min}$. We used the following criterion to determine $t_{\max}$:

$$t_{\max} \sim \max\left\{ \frac{2\pi}{\omega''}, 10 \times \frac{2\pi}{\omega_{\min}} \right\}. \qquad (21)$$

Since desirably we should have $\omega'' \ll \omega_{\min}$, $t_{\max}$ is typically of the order of $t_{\max} \sim 2\pi/\omega''$. The number of time steps is $t_{\max}/\Delta_t$.

It is clear that the simulations will take longer for smaller values of ω''. On the other hand, small values of ω'' yield more accurate results. Indeed, we want to calculate the effective parameters for real valued frequencies $[\bar{\bar{\varepsilon}}_{\mathrm{eff}}(\omega',\mathbf{k})]$, but the result of the numerical calculation is actually $\bar{\bar{\varepsilon}}_{\mathrm{eff}}(\omega' + i\omega'',\mathbf{k})$. In all our simulations we used $\omega'' a/c = 0.001$, where a is the lattice constant of the metamaterial. We found that such a choice gives very accurate results. The typical number of time steps for a spatial grid with $N_x = N_y = N_z = 30$ ranges from 10^5 to 10^6.

C. Extraction of the local parameters

In case of metamaterials characterized by weak spatial dispersion, it is possible to extract the local parameters (e.g., local effective permittivity and permeability) from the nonlocal dielectric function by calculating derivatives of $\bar{\bar{\varepsilon}}_{\mathrm{eff}}(\omega,\mathbf{k})$ with respect to the wave vector.[4,5,14,15,21] Assuming that there is no magnetoelectric coupling, the local (relative) permittivity is given by[4,15]

$$\bar{\bar{\varepsilon}}(\omega) = \frac{1}{\varepsilon_0} \bar{\bar{\varepsilon}}_{\mathrm{eff}}(\omega,\mathbf{k}=0). \qquad (22)$$

On the other hand, if the effects of second-order spatial dispersion can be characterized by a permeability tensor (and if the effect of the quadrupole moment is negligible; see Ref. 5) the zz component of the permeability satisfies[4,15]

$$\frac{\mu_{zz}}{\mu_0} \equiv \mu_{r,zz}(\omega) = \frac{1}{1 - \left(\frac{\omega}{c}\right)^2 \frac{1}{2\varepsilon_0} \left.\frac{\partial^2 \varepsilon_{\mathrm{eff},yy}}{\partial k_x^2}\right|_{\mathbf{k}=0}}. \qquad (23)$$

The formulas for other components of the permeability can be obtained by considering permutations of the indices x, y, and z. In practice, the permeability is calculated by evaluating the $\mathbf{k}$ derivatives of $\bar{\bar{\varepsilon}}_{\mathrm{eff}}(\omega,\mathbf{k})$ using finite differences.

IV. NUMERICAL STUDY

In order to validate the time domain homogenization method, in the first example we consider a two-dimensional square array of dielectric cylinders. The lattice constant of the array is a, and the cylinders have radius $R = 0.4a$, permittivity $\varepsilon_d = 56.0$, and stand in host material with $\varepsilon_h = 1.0$. We have calculated the local effective parameters using Eqs. (22) and (23). It is important to emphasize that the calculation of the effective permeability μ (in this and in all the remaining examples of the paper) is done by calculating derivatives of the nonlocal dielectric function with respect to the wave vector, as in Eq. (23). In practice, this involves evaluating $\bar{\bar{\varepsilon}}_{\mathrm{eff}}(\omega,\mathbf{k})$ for nontrivial values of $\mathbf{k}$. Therefore the effective permeability can be regarded as a manifestation of weak spatial dispersion. On the other hand, the local permittivity is obtained from the nonlocal dielectric function by setting $\mathbf{k} = 0$, as in Eq. (22).
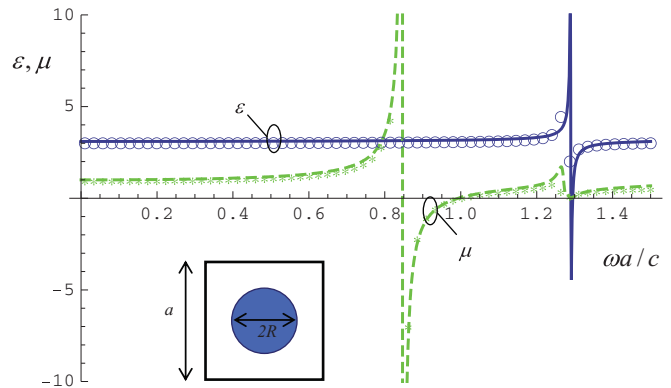
FIG. 1. (Color online) Effective permittivity and permeability as a function of the normalized frequency for an array of dielectric cylinders with $\varepsilon_d = 56.0$ and $R = 0.4a$. Solid lines: FDTD results; discrete symbols: FDFD method of Ref. 5. The inset shows the geometry of the unit cell.

In Fig. 1, we depict the effective permittivity and permeability as a function of frequency calculated with (i) the FDTD approach proposed here, and (ii) the FDFD method of Ref. 5 (discrete symbols). As can be seen, the agreement between both methods for this two-dimensional geometry is very good. Figure 1 shows that the metamaterial has a resonant magnetic response, which is a consequence of a Mie resonance in the high-permittivity inclusions.[22,23] This example clearly illustrates that even though the metamaterial is completely lossless, and that even though there is no radiation loss, the proposed time domain approach yields, indeed, convergent results. As explained in Sec. II, this is made possible by the fact that the effective parameters are evaluated in the upper-half plane, slightly above the real frequency axis. It is interesting to compare the computational efficiency of our FDTD scheme with the FDFD formulation of Ref. 5. For the present two-dimensional (2D) problem, and for a computational domain with 40×40 spatial nodes we found that the time domain simulation is three times faster than the corresponding FDFD simulation for a comparable number of frequency samples. We expect the efficiency to be dramatically improved for large scale three-dimensional problems (such problems are inaccessible to our nonoptimized implementation of the FDFD formalism; indeed, it is limited to about 4000 unknowns due to the fact that it calculates the solution of the pertinent linear system using the Gauss elimination method, without taking advantage of numerical methods to solve sparse linear systems). Nevertheless, it should be mentioned that the computational load of the frequency domain approach may be drastically reduced by using spectral estimation methods that may help predicting a wideband response from a few frequency samples. A detailed discussion of these aspects is, however, out of the intended scope of the present work.

In the second example, we consider a metamaterial that is known to be characterized by strong spatial dispersion in the long-wavelength limit: the "wire medium."[24] The material is formed by an array of metallic rods oriented along the z direction, with radius R, and arranged in a square lattice with period a. The metallic rods are characterized by a Drude-type dispersion model with $\varepsilon_m = 1 - \omega_p^2/\omega(\omega + i\Gamma)$. The
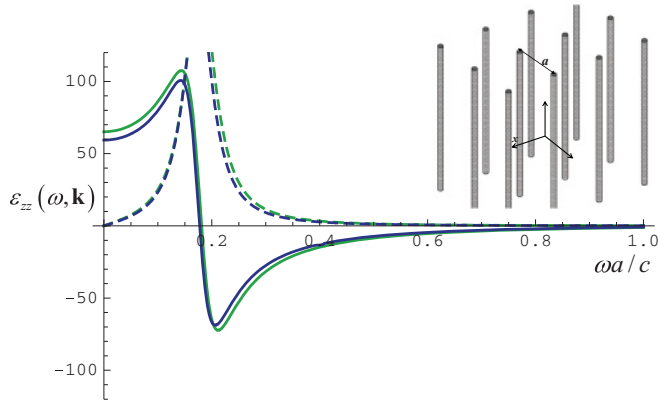
FIG. 2. (Color online) Nonlocal dielectric function $[\varepsilon_{zz}(\omega,\mathbf{k})]$ as a function of the frequency for the case $k_z = 0.1\pi/a$ and $k_x = k_y = 0$. Blue (darker) lines: FDTD results; green (lighter) lines: analytical model of Ref. 25. The solid lines represent the real part of the permittivity and the dashed lines the imaginary part. The inset shows the geometry of the metamaterial.

normalized plasma frequency is taken equal to $\omega_p a/c = 10.0$, and the collision frequency is such that $\Gamma = 0.01\omega_p$. In order to highlight the effects of spatial dispersion, and to demonstrate that our numerical method can capture these quite accurately, we have computed the z component $[\varepsilon_{zz}(\omega,\mathbf{k})]$ of the nonlocal dielectric function as a function of the frequency for the case $k_z = 0.1\pi/a$ and $k_x = k_y = 0$. The obtained results are depicted in Fig. 2 (blue lines). In the same figure we plot the value of $\varepsilon_{zz}(\omega,\mathbf{k})$ predicted by an available analytical model [green lines calculated using Eq. (16) of Ref. 25]. Notice that in the present example the inclusions are dispersive materials, and thus the homogenization method must be implemented as explained in the Appendix. As seen, the agreement between the full wave results and the analytical model is quite good. Notice that the effective permittivity for low frequencies is positive and extremely large. Quite differently, if one would neglect the effects of spatial dispersion (i.e., the dependence of the dielectric function on k_z), one would find that ε_{zz} would be negative and follow a Drude dispersion model. For more details about the effects of spatial dispersion in wire media the reader is referred to relevant works on this topic (e.g., Ref. 24).

In the next example, we consider a fully three-dimensional metamaterial formed by a simple cubic (sc) lattice of dielectric spheres with radius $R = 0.45a$ and permittivity $\varepsilon_d = 20.0$ standing in air ($\varepsilon_h = 1.0$). The calculated effective permittivity and permeability are plotted in Fig. 3 (solid lines), superposed on the results predicted by the well-known Lewin's formulas.[26] In the case of inclusions with a trivial magnetic response, Lewin's formulas may be written as follows:

$$\varepsilon_L = \varepsilon_h \left(1 + \frac{1}{a^3 \alpha_e^{-1} - 1/3}\right), \quad \mu_L = 1 + \frac{1}{a^3 \alpha_m^{-1} - 1/3},$$
(24)

where

$$\alpha_e^{-1} = \frac{1}{4\pi R^3} \frac{F(\theta) + 2\varepsilon_h/\varepsilon_d}{F(\theta) - \varepsilon_h/\varepsilon_d}, \quad \alpha_m^{-1} = \frac{1}{4\pi R^3} \frac{F(\theta) + 2}{F(\theta) - 1},$$
(25)
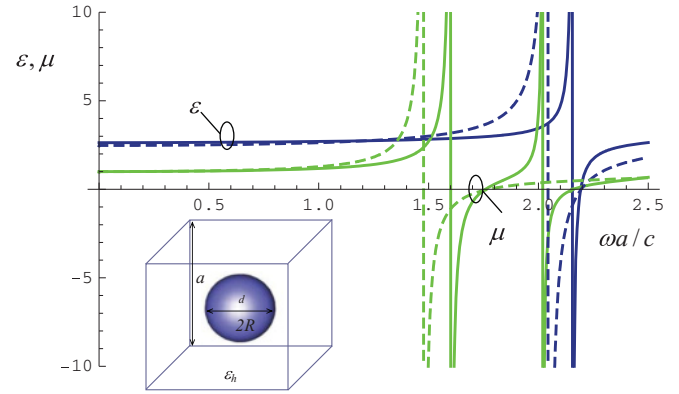
FIG. 3. (Color online) Effective permittivity and permeability as a function of frequency for a simple cubic array of dielectric spheres with $\varepsilon_d = 20.0$ and $R = 0.45a$ embedded in air. Solid lines: FDTD results; dashed lines: Lewin's formulas (Ref. 26). The inset shows the geometry of the unit cell.

with $F(\theta) = 2(\sin\theta - \theta\cos\theta)/[(\theta^2 - 1)\sin\theta + \theta\cos\theta]$ and $\theta = (\omega R/c)\sqrt{\varepsilon_d}$, ε_d being the permittivity of the spherical inclusions and ε_h the permittivity of the host material.[26] It is seen in Fig. 3 that while for relatively low frequencies the agreement between the full wave results and Lewin's mixing formula is excellent, there is some disagreement close to the resonances of the permittivity and permeability, and in particular Lewin's formula—being quasistatic in nature—fails to predict the second resonance of the permeability. This second resonance is therefore due to the interaction between the dielectric particles (effect of periodicity).

In the previous examples both the permittivity and the permeability may be negative over some frequency band, but unfortunately such bands do not overlap. There is, however, a quite interesting possibility of designing matched double negative materials based on permittivity near zero (ENZ) materials.[27] In fact, in a previous work[28] it was shown that by embedding dielectric particles in a ENZ host it is possible to tune the permittivity of the inclusions in a such way that the effective medium has simultaneously near zero permittivity and permeability. Hence because of causality constraints, this implies that for frequencies below the plasma frequency the effective parameters are simultaneously negative. Even though the geometry considered in Ref. 27 was intrinsically two dimensional, next we demonstrate with the help of our time domain homogenization formalism that the same ideas also hold in the three-dimensional case. To this end, we consider a sc lattice of dielectric spheres with radius $R = 0.4a$ and permittivity ε_d embedded in a host material such that the permittivity has a Drude-type dispersion: $\varepsilon_h = \varepsilon_\infty[1 - \omega_p^2/\omega(\omega + i\Gamma)]$. The normalized plasma frequency is taken equal to $\omega_p a/c = 1.0$, and to begin with the effect of loss is neglected, $\Gamma = 0$. It is clear that at the plasma frequency $\omega = \omega_p$ (ENZ regime) the effective medium is also characterized by a zero effective permittivity.[27] In order that the effective permeability also vanishes at the same frequency, we used Lewin's formula for the permeability (24) to tune the permittivity of the inclusions. Assuming $R = 0.4a$, this gives us $\varepsilon_d = 73.1$. We used $\varepsilon_\infty = 3.6$ in our simulations because we checked with Lewin's formulas that this would ensure
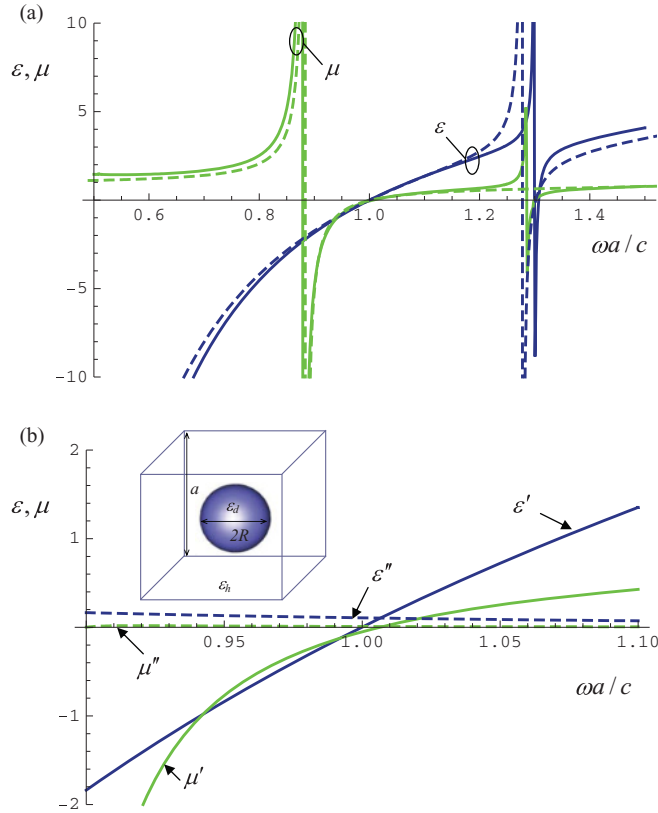
FIG. 4. (Color online) Effective permittivity $\varepsilon = \varepsilon' + i\varepsilon''$ and effective permeability $\mu = \mu' + i\mu''$ as a function of frequency for a simple cubic array of dielectric spheres with $\varepsilon_d = 73.1$ and $R = 0.4a$ embedded in a plasmonic host. Panel (a) Lossless case; solid lines: FDTD results; dashed lines: Lewin's formulas (Ref. [26]). Panel (b) Zoom of panel (a) but for a lossy host with $\Gamma/\omega_p = 0.019$.

FIG. 5. (Color online) Effective permittivity and permeability as a function of frequency for a simple cubic array of dielectric spheres with $\varepsilon_d = 56.0$ and $R = 0.4a$ embedded in a plasmonic host. Solid lines: FDTD results; dashed lines: Lewin's formulas (Ref. [26]).

that $\varepsilon_L \approx \mu_L$ (matched index material) over a broad range of frequencies close to $\omega = \omega_p$.

The computed effective parameters are shown in Fig. 4(a) (solid lines), superposed on the curves obtained using Lewin's theory (dashed lines). The results of Fig. 4(a) reveal a formidable agreement between Lewin's theory and our full wave time domain homogenization, particularly near $\omega = \omega_p$. Moreover, close to $\omega = \omega_p$ the metamaterial behaves as a matched index material and the conditions $\varepsilon = \mu = -1$ are observed simultaneously, which indicates that the metamaterial may behave to some extent as a Veselago-Pendry's lens.[1,29] These ideas will be further developed elsewhere.

It is important to emphasize that, unlike in the example of Fig. 3, in the case of an ENZ host Lewin's theory can be extremely accurate, even for relatively large frequencies of operation. The reason is actually quite simple to understand: In an ENZ material we have $\varepsilon_h \approx 0$ and hence the wavelength in the host material is extremely large. As a consequence, the interaction between the inclusions is inherently quasistatic and hence the effective parameters are accurately modeled by Lewin's formulas. It is also interesting to observe that despite the absence of loss mechanisms in the host material (with a Drude-type dispersion), the FDTD simulations yield convergent results.

We have also studied the effect of loss in the host material on the effective parameters of the metamaterial. This study is reported in Fig. 4(b), at the frequency window where both the permittivity and permeability are simultaneously negative. In the simulations it was assumed that the host material is characterized by a collision frequency such that $\Gamma/\omega_p = 0.019$. It is seen in Fig. 4(b) that the effect of absorption on the effective parameters is very moderate, particularly the effect on the permeability is practically negligible.

In order to demonstrate the extraordinary design potentials of metamaterials based on an ENZ host material, in Fig. 5 we study the scenario where dielectric spheres with $R = 0.4a$ and $\varepsilon_d = 56.0$ are embedded in a host with $\varepsilon_\infty = 1.0$, $\Gamma/\omega_p = 0$, and $\omega_p a/c = 1.0$. In this example, the permittivity of the inclusions was tuned using Lewin's formulas so that $\varepsilon_{\mathrm{eff}} = 0$ and $\mu_{\mathrm{eff}} = \infty$ at the plasma frequency of the host material. As seen in Fig. 5, even in this extreme scenario the full wave FDTD results agree extremely well with Lewin's formulas. Therefore an important conclusion of this study is that Lewin's formulas may be regarded as nearly exact in case of an ENZ host.

In the last example, in order to illustrate the generality and robustness of our method, we consider a fishnet metamaterial. The geometry of unit cell is shown in the inset of Fig. 6. The parameters of the metamaterial are taken from Ref. [30], which reported the emergence of negative refraction in the optical domain: transverse period $a = 860$ nm, longitudinal period $p = 80$ nm, thickness of the silver (Ag) layers $p_{\mathrm{Ag}} = 30$ nm, thickness of the magnesium fluoride (MgF$_2$) layers $p_{\mathrm{MgF}_2} = 50$ nm, and y and z widths of the fishnet $w_y = 565$ nm and $w_z = 265$ nm. The Ag and MgF$_2$ layers stand in air. Following Ref. [30], the permittivity of silver is modeled by a Drude dispersion model with $\omega_p/2\pi = 2173$ THz and $\Gamma/\omega_p = 0.006$. The index of refraction of MgF$_2$ is taken equal to $n = 1.38$.

In Fig. 6(a) we depict the calculated effective permittivity (ε_{yy}) and permeability (μ_{zz}) as a function of frequency. Consistent with the results of Ref. [30], it is seen that in the band 160 THz $< f <$ 200 THz the effective parameters are simultaneously negative. In Fig. 6(b) we compare the real part of the index of refraction $n_{\mathrm{eff}} = \sqrt{\varepsilon\mu}$ calculated with our homogenization approach (solid line), with data
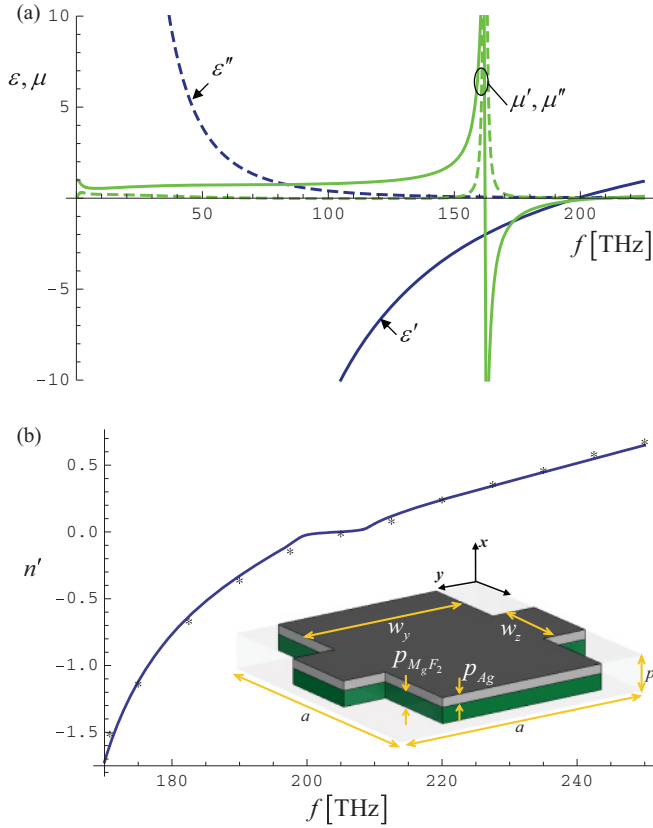
FIG. 6. (Color online) (a) Effective permittivity $\varepsilon_{yy} = \varepsilon' + i\varepsilon''$ and effective permeability $\mu_{zz} = \mu' + i\mu''$ of a fishnet metamaterial as a function of frequency. (b) Solid line: real part of the index of refraction as a function of frequency (propagation is along the x direction); Discrete symbols: data extracted from Ref. 30. The inset shows the geometry of the unit cell.

extracted from Fig. 3(b) of Ref. 30 (star-shaped symbols) obtained with a "rigorous coupled wave analysis" (RCWA). As seen, the agreement is remarkably, and perhaps surprisingly, good. In particular, our effective-medium theory completely supports the findings of Ref. 30 and the emergence of negative refraction. It is, however, important to mention that μ calculated using Eq. (23) can be regarded as the local permeability only in the case of weak spatial dispersion, and assuming that the contribution of the quadrupole moment is negligible. In general, these conditions may not be satisfied by the fishnet structure due to spatial dispersion effects,[31–33] and thus μ may depend on the direction of propagation in the metamaterial[5] losing its meaning as a true mesoscopic parameter. This important issue is out of the scope of this paper and will be analyzed in detail elsewhere.

V. CONCLUSION

In this work, building on our previous works,[4,5] we developed a time domain approach to characterize the effective parameters of metamaterials. The method is based on the excitation of the metamaterial with an external current source. Alternatively, instead of considering an external source as assumed here, the effective parameters could also be obtained by assuming that the initial time boundary conditions are of

the form $\mathbf{h}(t=0)=0$ and $\mathbf{d}(t=0) \sim e^{i\mathbf{k} \cdot \mathbf{r}}$, where $\mathbf{d}$ is the microscopic electric displacement vector. Unlike frequency domain methods, the computational effort of our approach scales linearly with the size of the computational domain (number of nodes in the mesh), and thus it provides an efficient, rigorous, and general approach to the homogenization of arbitrary fully three-dimensional metamaterials. The proposed algorithm can be very easily implemented in existing FDTD electromagnetic solvers. An important finding of this paper is that metamaterials based on an ENZ host with dielectric inclusions enable a regime of relatively low loss and matched impedance operation, with the effective permittivity and permeability simultaneously negative. Furthermore, such metamaterials can be modeled very accurately using Lewin's mixing formulas. Our time domain homogenization formalism can be easily adapted to the study of nonlinear metamaterials.

APPENDIX: THE FREQUENCY DISPERSIVE CASE

In this Appendix, we discuss the general case where the permittivity of the inclusions is frequency dispersive. Let us suppose that the complex (microscopic) permittivity of the system is of the form

$$\varepsilon(\mathbf{r}; \omega) = \varepsilon_s(\mathbf{r}) - \frac{\sigma}{i\omega} + \varepsilon_0 \chi_d(\mathbf{r}; \omega), \quad (A1)$$

where ε_s is the "static" component of the permittivity (independent of frequency), $\sigma = \sigma(\mathbf{r})$ is the conductivity, and χ_d is the frequency-dependent part of the susceptibility. For simplicity, we only discuss the scenario where $\chi_d(\mathbf{r}; \omega) = -\omega_p^2/[\omega(\omega + i\Gamma)]$, which is adequate to model inclusions with a Drude-type dispersion model. The parameters $\omega_p = \omega_p(\mathbf{r})$ and $\Gamma = \Gamma(\mathbf{r})$ are the usual plasma and collision frequencies, respectively. They are position dependent, and should be set equal to zero in dielectric regions (i.e., in regions where $\chi_d = 0$). The general case where χ_d is a rational function of frequency (e.g., a Lorentz dispersion model) can be treated similarly to the Drude case.

In order to formulate the homogenization problem in the time domain it is necessary to introduce an auxiliary field $\mathbf{v}_1$ that describes the dynamics of the response of the microscopic dielectric function in terms of a differential equation. The problem to be solved in the time domain is now (this is similar to the approach of Ref. 34)

$$\nabla \times \mathbf{e} = -\mu_0 \frac{\partial \mathbf{h}}{\partial t}, \quad (A2a)$$

$$\nabla \times \mathbf{h} = \mathbf{j}_e + \sigma(\mathbf{r})\mathbf{e} + \varepsilon_s(\mathbf{r})\frac{\partial \mathbf{e}}{\partial t} + \varepsilon_0 \omega_p^2(\mathbf{r})\mathbf{v}_1, \quad (A2b)$$

$$\frac{\partial \mathbf{v}_1}{\partial t} + \Gamma \mathbf{v}_1 = \mathbf{e}. \quad (A2c)$$

Therefore there are three unknown vector fields: $\mathbf{e}$, $\mathbf{h}$, $\mathbf{v}_1$. All the unknowns need to be discretized in the FDTD solution. The initial time conditions are taken as

$$\mathbf{e}(\mathbf{r},t=0) = 0 \quad \mathbf{h}(\mathbf{r},t=0) = 0,$$
$$\mathbf{v}_1(\mathbf{r},t=0) = 0 \tag{A3}$$

It can be easily checked that in the Laplace domain the electric and magnetic fields satisfy

$$\nabla \times \tilde{\mathbf{e}} = -\mu_0 s \tilde{\mathbf{h}}, \tag{A4a}$$
$$\nabla \times \tilde{\mathbf{h}} = \tilde{\mathbf{j}}_e + s\varepsilon(\mathbf{r};s)\tilde{\mathbf{e}}, \tag{A4b}$$

where $\varepsilon(\mathbf{r};s)$ is defined as in Eq. (A1) with $s = -i\omega$. This justifies the definition of the auxiliary field $\mathbf{v}_1$.

The averaged polarization vector in the time domain must now be defined as

$$\mathbf{P}_{g,\mathrm{av}}(t) = \frac{1}{V_{\mathrm{cell}}} \int_\Omega (\varepsilon_s - \varepsilon_0)\mathbf{e}(\mathbf{r},t)e^{-i\mathbf{k}\cdot\mathbf{r}}d^3\mathbf{r}$$
$$+ \mathbf{W}_1(t) + \mathbf{W}_2(t), \tag{A5}$$

where

$$\mathbf{W}_m(t) = \int_0^t \mathbf{V}_m(t)dt \quad (m=1,2) \tag{A6}$$

and

$$\mathbf{V}_1(t) = \frac{1}{V_{\mathrm{cell}}} \int_\Omega \varepsilon_0 \omega_p^2(\mathbf{r})\mathbf{v}_1(\mathbf{r},t)e^{-i\mathbf{k}\cdot\mathbf{r}}d^3\mathbf{r}, \tag{A7}$$

$$\mathbf{V}_2(t) = \frac{1}{V_{\mathrm{cell}}} \int_\Omega \sigma(\mathbf{r})\mathbf{e}(\mathbf{r},t)e^{-i\mathbf{k}\cdot\mathbf{r}}d^3\mathbf{r}. \tag{A8}$$

Notice that the Laplace transform of $\mathbf{P}_{g,\mathrm{av}}(t)$ satisfies

$$\tilde{\mathbf{P}}_{g,\mathrm{av}}(s) = \frac{1}{V_{\mathrm{cell}}} \int_\Omega [\varepsilon(\mathbf{r};s) - \varepsilon_0]\tilde{\mathbf{e}}(\mathbf{r},s)e^{-i\mathbf{k}\cdot\mathbf{r}}d^3\mathbf{r}, \tag{A9}$$

which justifies the form of Eq. (A5).

The effective dielectric function can be determined from $\mathbf{P}_{g,\mathrm{av}}(t)$ and $\mathbf{E}_{\mathrm{av}}(t)$, exactly in the same manner as explained in section II. The FDTD discretization of system (A2) is analogous to that of Sec. III. The auxiliary field $\mathbf{v}_1$ is discretized at the same spatial and time nodes as the electric field. The time discretization of Eq. (A2c) is done as follows:

$$\mathbf{v}_1^{n+1}(\mathbf{r}) = \frac{\Delta_t}{1 + \Gamma(\mathbf{r})\Delta_t/2} \mathbf{e}^n(\mathbf{r}) + \mathbf{v}_1^n(\mathbf{r})\frac{1 - \Gamma(\mathbf{r})\Delta_t/2}{1 + \Gamma(\mathbf{r})\Delta_t/2}, \tag{A10}$$

where $\mathbf{v}_1^n(\mathbf{r}) = \mathbf{v}_1(\mathbf{r},n\Delta_t)$, etc. On the other hand, Eq. (16) should be replaced by [20]

$$e_z^{n+1}\left(i,j,k+\frac{1}{2}\right)$$

$$= \frac{1 - q\left(i,j,k+\frac{1}{2}\right)\Delta_t/2}{1 + q\left(i,j,k+\frac{1}{2}\right)\Delta_t/2} e_z^n\left(i,j,k+\frac{1}{2}\right) + \frac{1}{1 + q\left(i,j,k+\frac{1}{2}\right)\Delta_t/2} \frac{\Delta_t}{\varepsilon_s\left(i,j,k+\frac{1}{2}\right)}$$

$$\times \left[-j_{e,z}^{n+1/2}\left(i,j,k+\frac{1}{2}\right) - \varepsilon_0\omega_p^2\left(i,j,k+\frac{1}{2}\right)v_{1,z}^{n+1}\left(i,j,k+\frac{1}{2}\right) \right.$$

$$\left. + \frac{h_y^{n+1/2}\left(i+\frac{1}{2},j,k+\frac{1}{2}\right) - h_y^{n+1/2}\left(i-\frac{1}{2},j,k+\frac{1}{2}\right)}{\Delta_x} - \frac{h_x^{n+1/2}\left(i,j+\frac{1}{2},k+\frac{1}{2}\right) - h_x^{n+1/2}\left(i,j-\frac{1}{2},k+\frac{1}{2}\right)}{\Delta_y} \right], \tag{A11}$$

where $q = \sigma/\varepsilon_s$. Finally, Eq. (A6) may be discretized as follows:

$$\mathbf{W}_m^{n+1} = \mathbf{W}_m^n + \Delta_t \mathbf{V}_m^n, \, (m=1,2), \tag{A12}$$

where $\mathbf{W}_m^n = \mathbf{W}_m(n\Delta_t)$ and $\mathbf{V}_m^n = \mathbf{V}_m(n\Delta_t)$.

*mario.silveirinha@co.it. pt

[1] J. B. Pendry, Phys. Rev. Lett. **85**, 3966 (2000).

[2] M. G. Silveirinha, Phys. Rev. Lett. **102**, 193903 (2009).

[3] J. B. Pendry, A. J. Holden, D. J. Robbins, and W. J. Stewart, IEEE Trans. Microwave Theory Tech. **47**, 2075 (1999).

[4] M. G. Silveirinha, Phys. Rev. B **75**, 115104 (2007).

[5] J. T. Costa, M. G. Silveirinha, and S. I. Maslovski, Phys. Rev. B **80**, 235124 (2009).

[6] G. Milton, *The Theory of Composites* (Cambridge University Press, Cambridge, England, 2001).

[7] C. R. Simovski and S. A. Tretyakov, Phys. Rev. B **75**, 195111 (2007);] C. R. Simovski, Metamaterials **1**, 62 (2008).

[8] D. R. Smith and J. B. Pendry, J. Opt. Soc. Am. B **23**, 391 (2006).

[9] D. R. Smith, Phys. Rev. E **81**, 036605 (2010).

[10] W. L. Mochán and R.G. Barrera, Phys. Rev. B **32**, 4984 (1985).

[11] G. P. Ortiz, B. E. Martínez-Zérega, B. S. Mendoza, and W. L. Mochán, Phys. Rev. B **79**, 245132 (2009).

[12] A. Alu, e-print arXiv:1012.1351 (to be published).

[13] C. Fietz and G. Shvets, Physica B **405**, 2930 (2010).

[14] M. G. Silveirinha, Phys. Rev. B **80**, 235120 (2009).

[15] M. G. Silveirinha, *Theory and Phenomena of Metamaterials*, edited by F. Capolino, Handbook of Artificial Materials (CRC Press, Boca Raton, 2009).

[16] A. Taflove and S. C. Hagness, *Computational Electrodynamics: The Finite-Difference Time-Domain Method* (Artech House, London, 2005).

[17] K. S. Yee, IEEE Trans. Antennas Propagat. **14**, 302 (1966).

[18] A. J. Ward and J. B. Pendry, Phys. Rev. B **58**, 7252 (1998).

[19] C. T. Chan, Q. L. Yu, and K. M. Ho, Phys. Rev. B **51**, 16635 (1995).

[20] A. Taflove, Wave Motion **10**, 547 (1988).

[21] V. M. Agranovich, Y. R. Shen, R. H. Baughman, and A. A. Zakhidov, Phys. Rev. B **69**, 165112 (2004).

[22] S. O'Brien and J. B. Pendry, J. Phys.: Condens. Matter **14**, 4035 (2002).

[23] C. L. Holloway, E. F. Kuester, J. Baker-Jarvis, and P. Kabos, IEEE Trans. Antennas and Propag. **51**, 2596 (2003).

[24] P. A. Belov, R. Marqués, S. I. Maslovski, I. S. Nefedov, M. Silveirinha, C. R. Simovski, and S. A. Tretyakov, Phys. Rev. B **67**, 113103 (2003).

[25] M. G. Silveirinha, Phys. Rev. E **73**, 046612 (2006).

[26] L. Lewin, Proc. Inst. Elec. Eng. **94**, 65 (1947).

[27] M. Silveirinha and N. Engheta, Phys. Rev. Lett. **97**, 157403 (2006).

[28] M. G. Silveirinha and N. Engheta, Phys. Rev. B **75**, 075119 (2007).

[29] V. G. Veselago, Sov. Phys. Usp. **10**, 509 (1968).

[30] J. Valentine, S. Zhang, T. Zentgraf, E. Ulin-Avila, D. A. Genov, G. Bartal, and X. Zhang, Nature (London) **455**, 376 (2008).

[31] D. J. Cho, F. Wang, X. Zhang, and Y. R. Shen, Phys. Rev. B **78**, 121101(R) (2008).

[32] C. Menzel, T. Paul, C. Rockstuhl, T. Pertsch, S. Tretyakov, and F. Lederer, Phys. Rev. B **81**, 035320 (2010).

[33] L. Jelinek, R. Marques, and J. Machac, Opt. Express **18**, 17940 (2010).

[34] R. M. Joseph, S. C. Hagness, and A. Taflove, Opt. Lett. **16**, 1412 (1991).